RSC Advances

ROYAL SOCIETY OF CHEMISTRY

www.rsc.org/advances

Cite this: DOI: 10.1039/c0xx00000x

www.rsc.org/xxxxxx

ARTICLE TYPE

Design and synthesis of multifunctional traceable dendrimers for visualizing drug delivery

Anjali Sharma[a], Diana Mejía[b] , Dusica Maysinger*[b] and Ashok Kakkar*[a]

Received (in XXX, XXX) Xth XXXXXXXXX 20XX, Accepted Xth XXXXXXXXX 20XX

DOI: 10.1039/b000000x

A versatile platform to track transport of dendrimers with fluorescent labels in the core and a desired number of drug molecules at the periphery, is reported.

Multifunctional nanocarriers which can be strategically engineered to include a desired combination of therapeutic and imaging agents, and help determine their fate in drug delivery, constitute a topical area of research in nanomedicine.[1] Among several platforms that have been explored for biomedical applications, dendrimers have offered tremendous potential due to their unique architecture and synthetic build-up in a layer-by-layer fashion, leading to well-defined compositions.[2] These macromolecules have been extensively explored for biological applications by physically encapsulating or covalently linking therapeutic and imaging agents.[3] It is becoming increasingly clear that a better strategy may be to design multifunctional nanocarriers in which therapeutic and imaging task-performing units are strategically placed at well-defined sites. This would lead to highly efficient therapeutic nanoprobes with which the passage and accumulation of nanocarriers at the desired site could be visualized.[4] In developing such a multi-tasking nanostructure, it is important to have a control on spatial distribution of different units to i) maximize the number of covalently linked therapeutic agents, and ii) to protect the imaging moiety from being degraded quickly during its passage to the desired site. Towards this goal, we report a simple and versatile synthetic methodology to construct traceable dendrimers for the efficient delivery of active pharmaceutical agents, and which can act as robust intrinsic nanoprobes. We chose 2',4',5',7'-tetraiodofluorescein (TIF) as a model fluorescent agent for this study due to its ease in availability, and the presence of hydroxyl functional groups which could be modified to perform a variety of chemical reactions while retaining its properties. Using this fluorescent core, traceable dendrimers were synthesized by a combination of highly efficient Cu(I) catalyzed alkyne-azide click reaction (CuAAC)[5] and Steglich esterification[6]. This methodology allows facile construction of traceable dendrimers with functional surface groups, which can be further utilized to covalently link any desired active pharmaceutical agents. We chose α-lipoic acid (α-LA), an antioxidant and an endogenous cofactor for many enzymes,[7] as a model drug for this study. We demonstrate that these dendrimers are traceable, have comparable fluorescence intensities to commercially available TIF, are non-cytotoxic, and are internalized quickly by microglia (within minutes).

The synthesis of traceable dendrimers was initiated from 3,5-diacetylenebenzyl bromide **1**[8] on which two simultaneous click reactions were performed with 6-azidohexanoic acid to obtain an orthogonal motif **2** with two carboxylic acid moieties and a bromo focal point (Scheme **1**). It was followed by the conversion of bromide to an azide to afford compound **3**. In order to perform a click reaction on commercially available tetraiodofluorescein, its hydroxyl group was modified by carrying out an etherification reaction using propargyl bromide to obtain compound **4** (TIF_Mono_Acet, Scheme **1** and **S1**). It is important to note that only mono-propargylation of TIF should be carried out to retain its fluorescent properties, as dipropargylated derivative with propargylation at both hydroxyl and carboxylic acid positions, is non-fluorescent. Compound **3** was coupled to monopropargylated tetraiodofluorescein **4** *via* CuAAC click reaction.^{1}H NMR was used to follow the completion of this reaction with the disappearance of signal in the alkyne region together with the appearance of new signals for di-acid derivative and triazole H. Coupling of the resulting compound **5** with tripropargylated pentaerythritol **6** under Steglich conditions yielded fluorescent core **7** (TIF_6_Acet) with six acetylene arms. The structure of **7** was confirmed by ^{1}H and ^{13}C NMR as well as high resolution electrospray mass spectroscopy. 2-Azido ethanol was then clicked on compound **7** which resulted in the formation of dendrimer **8** (TIF-6_OH, Scheme **1**). The reaction was monitored by the appearance of triazole protons at 7.98 ppm in ^{1}H NMR. Subsequent esterification of **8** with α-lipoic acid provided the desired dendrimer-drug conjugate **9** (TIF_6_LA). ^{1}H NMR indicated a shift in methylene protons next to hydroxyl groups with the appearance of additional signals for lipoic acid protons.

In order to demonstrate the versatility of this methodology, the synthesis was further elaborated to next generation traceable dendrimer with 12 hydroxyl groups. The building block **10** was synthesized by reacting compound **1** with 2-azido ethanol using click chemistry (Scheme **2**). The bromide functional group on **10** was subsequently converted to an azide to afford compound **11**. The coupling of azide terminated dihydroxy building block **11** on fluorescent core **7** using CuAAC click reaction resulted in the formation of dodecahydroxy compound **12** (TIF-12-OH). This methodology can be subsequently repeated to construct the next generation dendrimer by clicking compound **11** on to **1**, and then following the steps as outlined in Scheme **2**. We also constructed

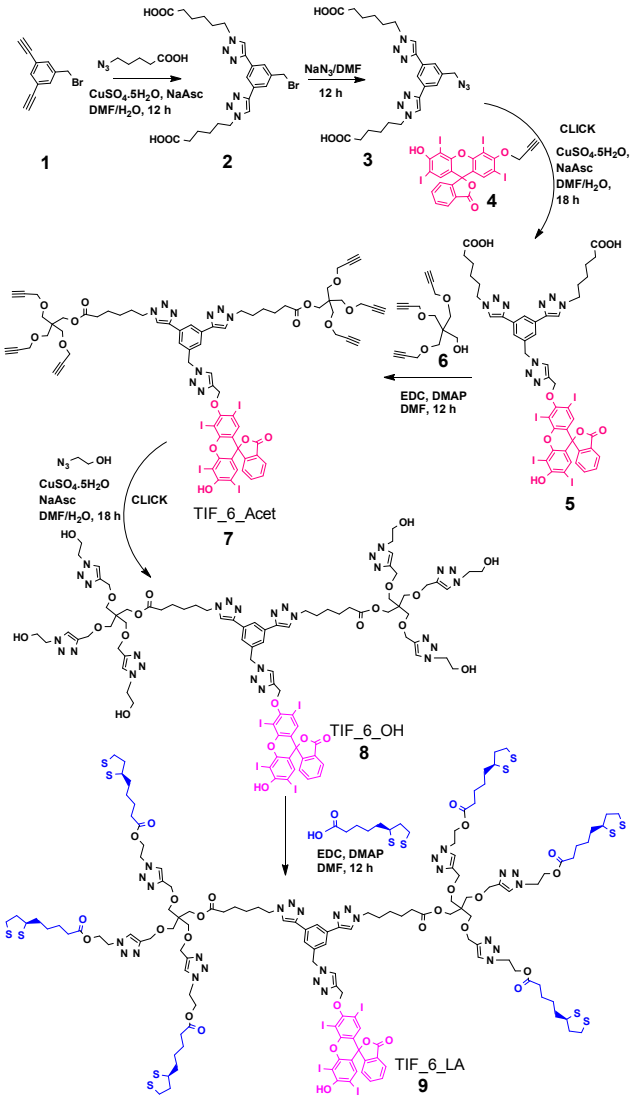

Scheme 1 Schematic representation for construction of hydroxyl terminated traceable dendrimer **8**(TIF_6_OH), and its conjugation to α-lipoic acid to give dendrimer **9**(TIF_6_LA).

hydroxyl terminated linear counterpart (**13**, Scheme **S1**) of the dendrimers by the click reaction of monopropargylated tetraiodofluorescein **4** with 2-azido ethanol.

UV-Vis absorption spectra of free TIF as well as all fluorescent conjugates containing TIF dye, were recorded to determine their photophysical properties. The absorption and emission spectra of fluorescent intermediates and dendrimers are shown in Figure **S1**. TIF absorbs around 530 nm and emits at 540 in methanol. The monopropargylated derivative **4** showed a red shift with an absorption around 540 nm, and emission at 560. All other fluorescent intermediates and dendrimers showed similar shifts around 10nm in absorption and 20 nm in emission as compared to free TIF (Figure **S1**). The fluorescent conjugates gave similar quantum yields as tetraiodofluorescein, showing no change in photophysical properties upon chemical modification of the dye, except in the case of TIF_12_OH (**12**). In the latter case, the quantum yield was lower (□7%) as compared to free TIF (15-17%, Table **S1**).

To explore the properties of the constructs in contact with

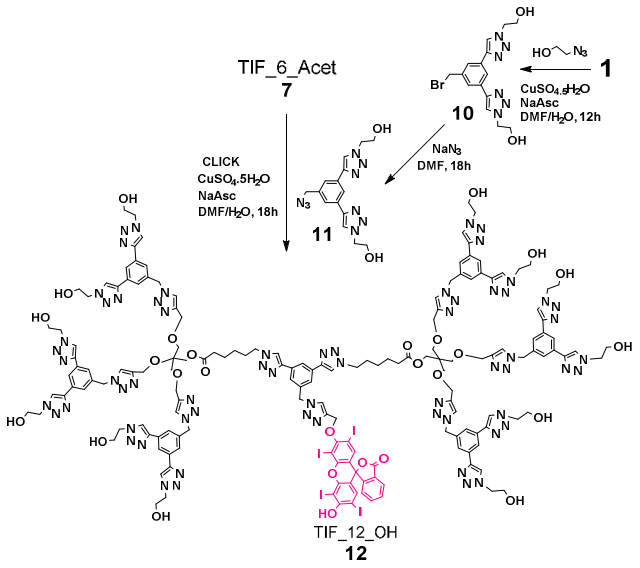

Scheme 2 Synthesis of traceable dendrimer **12** with 12 hydroxyl surface groups.

cells, biological experiments were carried out with peripheral and central nervous system (CNS) macrophages, namely J774A.1 macrophages and N9 microglia. Microglia are the immune cells of the CNS and the first line responders to insult. They play a critical role in maintaining brain homeostasis.[9] Conversely, depending on the extent of their activation, microglia can also impair neuronal functions. This activation is often related to their avidity to internalize certain biological materials (*e.g.* damaged cells, bacteria) and synthetic materials such as nanostructured particles (quantum dots, gold and polymeric nanoparticles).

The first aim of our biological studies was to show if the multifunctional nanocarriers are toxic, or can be considered harmless to microglia and macrophages. To this end, the mitochondrial activity of N9 microglia was assessed using an MTT assay since an impaired mitochondrial function is an indicator of cell viability. Microglia were exposed for 6 and 24 hours to TIF_6_OH (**8**, Figure **S2A**). No significant change in the metabolic activity was observed. Since the shorter treatments (6 hours) might not be adequate for detecting the mitochondrial damage, macrophages were treated with dendrimers (TIF_6_OH (**8**), TIF_12_OH (**12**), TIF_6_Acet (**7**)) for 24 hours (Figure **S2B**). Treatment of macrophages with dendrimers in concentrations up to 1 μM had no significant effect on the mitochondrial activity of the cells. Representative bright field images reveal no morphological changes in exposed cells (Figure **S2C**).

The uptake experiments were subsequently performed to explore the rate and extent of dendrimer internalization by microglia. Microglia were exposed to fluorescent structures (**TIF, 4, 13**) for 0-60 min and relative fluorescence intensity (RFI) was measured as a percentage of untreated control cells using a spectrofluorometer (ex 544/ em 590). Results from these studies suggest quick, time dependent internalization plateauing in fluorescence intensity within 40-60 minutes (Figure **1A**). RFI of fluorescent dendrimers (**7, 8, 12**) fell within the range of TIF dye and its analogs (**4** and **13**), indicating that the fluorescence and internalization of the constructs are detectable and comparable to

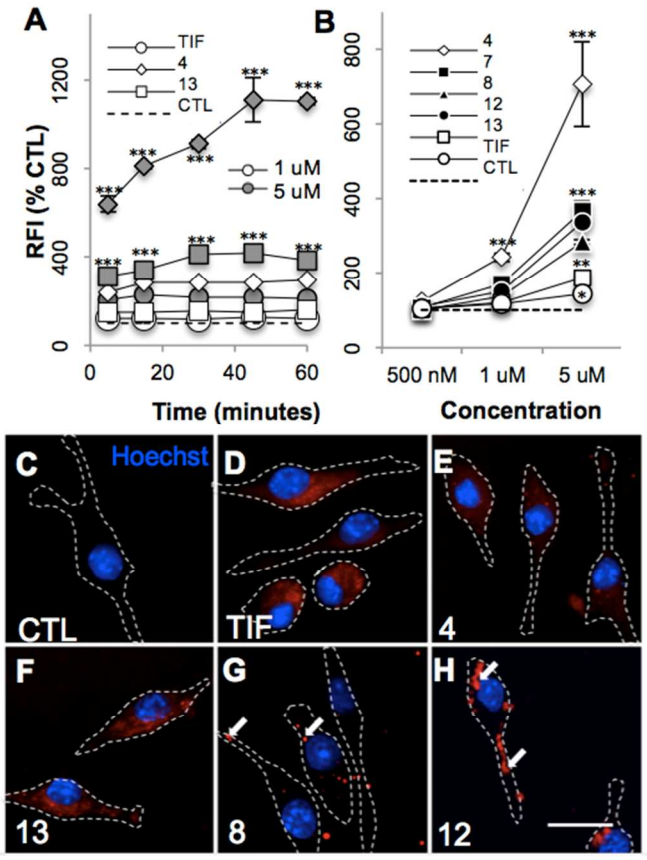

Fig. 1 Fluorescent dyes and dendrimers are internalized by microglia in a time and concentration dependent manner. Microglia were treated with fluorescent dye (TIF), its analogues (1μM, open markers or 5μM, shaded markers) or dendrimers (500nM-5μM) for 90 minutes, or as indicated. At the end of the experiment relative fluorescence intensity (RFI) was measured and presented as a percentage of untreated cells (CTL) **(A, B)**. Cells were fixed and nuclei stained with Hoechst 33342 (10 uM, 10 min). Confocal images of treated microglia were acquired to confirm dendrimer internalization and cellular location. Representative images of microglia treated with **C)** Control, **D)** TIF, **E)** TIF_Mono_Acet (4), **F)** TIF_Mono_OH (13), **G)** TIF_6_OH (8), and H) TIF-12-OH (12) (5μM, 90 min) are shown. Note the fluorescence in the soma and the cell extensions. Scale bar represents 20nm.

regular dyes in microglial cells after 90 minutes of treatment (Figure **1B**). Representative images of internalized dendrimers were acquired using confocal microscope. Cells were exposed to fluorescent structures (**7, 12**) for 90 min, fixed and nuclei were labeled with Hoechst 33342 (10uM, 10 min). TIF_12_OH (**12**) can be seen within microglial soma and the extensions, suggesting dendrimer agglomeration and compartmentalization within the cell. Z-stacks confirm nanoparticle internalization in microglial cells (Figure **S3A-C**). Confocal imaging of TIF_6_OH (**8**, Figure **1G**) and TIF_12_OH (**12**, Figure **1H**) suggest that different dendrimers agglomerate to different degrees within the cells, making the dendrimers versatile platforms for drug delivery paradigms. In contrast to the punctate dendrimer uptake distribution, free dye and its analogs (**TIF, 4** and **13**) remain diffused within microglia.

Multifunctional traceable dendrimers are efficiently internalized by microglia and do not cause any marked morphological or functional impairments. Imaging live cells exposed to the fluorescent dendrimers is easily achieved and shows their compartmentalization within cell soma and dendritic extensions. These properties, combined with the versatility of their synthesis, makes inherently fluorescent dendrimers promising tools for the development of traceable drug-delivery systems.

We would like to thank Natural Sciences and Engineering Research Council of Canada, (NSERC), Canadian Institutes of Health Research (CIHR) and Fonds de Recherche en Santé du Québec (FRSQ) and Centre for Self-Assembled Chemical Structures (FQRNT, Quebec, Canada) for financial support.

Notes and references

[a]*Department of Chemistry, McGill University, 801 Sherbrooke St. West, Montreal, Quebec, H3A 0B8, Canada. E-mail: ashok.kakkar@mcgill.ca; Fax: +514-398-3797; Tel: 514-398-6912*
[b]*Department of Pharmacology and Therapeutics, McGill University, 3655 Promenade Sir-William-Osler, Montreal, Quebec, H3G 1Y6, Canada. E-mail: Dusica.maysinger@mcgill.ca; Fax: +514-398-6690; Tel: +514-398-1264*[a]

† Electronic Supplementary Information (ESI) available: Details of studies related to photophysical properties, biology, synthesis, characterization, materials and methods, are provided as ESI. See DOI: 10.1039/b000000x

1 (a) S. Svenson, *Mol. Pharm.*, 2013, **10**, 848-856;(b) R. R. Sawant and V. P. Torchilin, *Curr. Opin. Solid State Mater. Sci.*, 2012, **16**, 269-275;(c) Z. Xu, B. He, J. Shen, W. Yang and M. Yin, *Chem. Commun.*, 2013, **49**, 3646-3648;(d) J. Zhang, G. Drugeon and N. L'Hermite, *Tetrahedron Lett.*, 2001, **42**, 3599-3601.
2 (a) J. Khandare, M. Calderon, N. M. Dagia and R. Haag, *Chem. Soc. Rev.*, 2012, **41**, 2824-2848;(b) G. M. Soliman, A. Sharma, D. Maysinger and A. Kakkar, *Chem. Commun.*, 2011, **47**, 9572-9587;(c) D. A. Tomalia and J. M. J. Fréchet, *J. Polym. Sci., Part A: Polym. Chem.*, 2002, **40**, 2719-2728;(d) R. Hourani and A. Kakkar, *Macromol. Rapid Commun.*, 2010, **31**, 947-974;(e) C. J. Hawker and J. M. J. Frechet, *J. Am. Chem. Soc.*, 1990, **112**, 7638-7647.
3 (a) L. M. Kaminskas, V. M. McLeod, C. J. H. Porter and B. J. Boyd, *Mol. Pharm.*, 2012, **9**, 355-373;(b) S. Parveen, R. Misra and S. K. Sahoo, *Nanomed-Nanotechnol.*, 2012, **8**, 147-166;(c) A. Sharma, A. Khatchadourian, K. Khanna, R. Sharma, A. Kakkar and D. Maysinger, *Biomaterials*, 2011, **32**, 1419-1429. (d) Y. Li, M.D. Giles, S. Liu, B.A. Laurent, J.N. Hoskins, M.A. Cortez, S.G. Sreerama, B.C. Gibb and S.M. Grayson, *Chem. Commun.*, 2011, **47**, 9036-9038.
4 (a) P. Prabhu and V. Patravale, *J. Biomed.l Nanotechnol,*, 2012, **8**, 859-882;(b) S. Mura and P. Couvreur, *Adv. Drug Deliver. Rev.*, 2012, **64**, 1394-1416;(c) A. M. Nyström and K. L. Wooley, *Acc. Chem. Res.*, 2011, **44**, 969-978.
5 (a) H. C. Kolb, M. G. Finn and K. B. Sharpless, *Angew. Chem. Int. Ed.*, 2001, **40**, 2004-2021;(b) G. Franc and A. K. Kakkar, *Chem. Soc. Rev.*, 2010, **39**, 1536-1544. (c) C.W. Tornoe, C. Christensen and M. Meldel, *J. Org. Chem.*, 2002, **67**, 3057-3064.
6 B. Neises and W. Steglich, *Angew. Chem. Int. Ed.*, 1978, **17**, 522-524.
7 L. Rochette, S. Ghibu, C. Richard, M. Zeller, Y. Cottin and C. Vergely, *Mol. Nutr. Food Res.*, 2013, **57**, 114-125.
8 R. Hourani, A. Sharma and A. Kakkar, *Tetrahedron Lett.*, 2010, **51**, 3792-3795.
9 A. Nimmerjahn, F. Kirchhoff and F. Helmchen, *Science*, 2005, **308**, 1314-1318.

Design and synthesis of multifunctional traceable dendrimers for visualizing drug delivery

Anjali Sharma, Diana Mejía, Dusica Maysinger* and Ashok Kakkar*

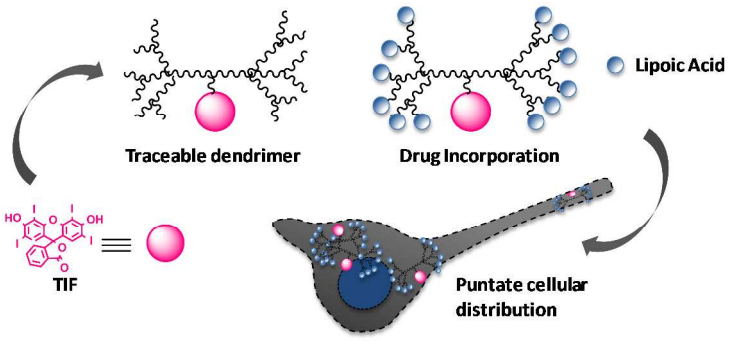

Multifunctional dendrimers with fluorescent molecules at the core light up cell compartments upon uptake.